Epithelial neoplasia in *Drosophila* entails switch to primitive cell states

Sumbul J. Khan[1,2], Anjali Bajpai[1], Mohammad Atif Alam[1,3], Ram P. Gupta, Sneh Harsh, Ravi K. Pandey, Surbhi Goel-Bhattacharya[4], Aditi Nigam, Arati Mishra, and Pradip Sinha[5]

Department of Biological Sciences and Bioengineering, Indian Institute of Technology Kanpur, Kanpur 208 016, India

Edited by Matthew P. Scott, Stanford University, Howard Hughes Medical Institute, Stanford, CA, and approved April 25, 2013 (received for review July 25, 2012)

Only select cell types in an organ display neoplasia when targeted oncogenically. How developmental lineage hierarchies of these cells prefigure their neoplastic propensities is not yet well-understood. Here we show that neoplastic *Drosophila* epithelial cells reverse their developmental commitments and switch to primitive cell states. In a context of alleviated tissue surveillance, for example, loss of Lethal giant larvae (Lgl) tumor suppressor in the wing primordium induced epithelial neoplasia in its Homothorax (Hth)-expressing proximal domain. Transcriptional profile of proximally transformed mosaic wing epithelium and functional tests revealed tumor cooperation by multiple signaling pathways. In contrast, *lgl*$^{-}$ clones in the Vestigial (Vg)-expressing distal wing epithelium were eliminated by cell death. Distal *lgl*$^{-}$ clones, however, could transform when both tissue surveillance and cell death were compromised genetically and, alternatively, when the transcription cofactor of Hippo signaling pathway, Yorkie (Yki), was activated, or when Ras/EGFR signaling was up-regulated. Furthermore, transforming distal *lgl*$^{-}$ clones displayed loss of Vg, suggesting reversal of their terminal cell fate commitment. In contrast, reinforcing a distal (wing) cell fate commitment in *lgl*$^{-}$ clones by gaining Vg arrested their neoplasia and induced cell death. We also show that neoplasia in both distal and proximal *lgl*$^{-}$ clones could progress in the absence of Hth, revealing Hth-independent wing epithelial neoplasia. Likewise, neoplasia in the eye primordium resulted in loss of Elav, a retinal cell marker; these, however, switched to an Hth-dependent primitive cell state. These results suggest a general characteristic of "cells-of-origin" in epithelial cancers, namely their propensity for switch to primitive cell states.

It is now well-recognized that only specific cell types in a given developmental hierarchy transform neoplastically when targeted by oncogenic lesions. For example, in mice, upon loss of the APC tumor suppressor, only intestinal crypt stem cells display neoplastic transformation while the transit amplifying cells, which are derived from these crypt stem cells, do not (1). Identification of cancer cells of origin is immensely important because biology of an oncogenically targeted cell is likely to provide clues to cancer pathogenesis (reviewed in ref. 2). It is conceivable that ontogeny, meaning developmental history, plays a crucial role in determining neoplastic propensity of oncogenically targeted cells. However, why different cell types of an organ display distinct neoplastic propensities have not yet been answered. Links between ontogeny and oncogeny (neoplasia) could be interrogated in genetically tractable organisms like the fruit fly, *Drosophila*, which carries a set of highly conserved tumor suppressor genes and display neoplastic growth when mutated (3).

Choice of a model organ to uncover the links between ontogeny and oncogeny is guided by a clarity in our understanding of lineage hierarchy among its different cell types. Epithelial primordia of *Drosophila* adult organ, the so-called "imaginal discs," are particularly suitable in this respect. The wing imaginal disc, for example, is a composite organ primordium that gives rise to notum (dorsal thorax) and hinge of the adult wing from its proximal domain whereas the wing blade proper is derived from its distal (pouch) domain (Fig. 1 *A*–*C*). Distal (wing) cell fate is specified by the Vestigial (Vg) field selector (4) whereas EGFR signaling (5) and activities of the Teashirt (Tsh) field selector and a homeo-domain transcription factor, Homothorax (Hth) (6, 7), specify proximal cell fate. At early second-larval instar stage—that is, before its proximal-distal lineage separation—the wing primordium displays ubiquitous Hth expression (6, 7). During late-second and early-third instar larval stages, a signaling axis set up by expression of Notch (N) and its target Wingless (Wg) specify wing cell fate by activating Vg (4) and repressing Hth at the presumptive distal tip of the wing primordium (7). Subsequently, combined activities of Wg and Vg in the distal domain create short-range feed-forward signals in collaboration with Yorkie (Yki) (8), the transcription cofactor of the Hippo signaling pathway (reviewed in ref. 9), thereby recruiting neighboring proximal cells into an expanding distal (wing) field; the distal wing is thus carved out of a Hth-expressing ground state. It has also been seen that when wing cell fate is not specified, for example in the absence of distal Wg signaling, presumptive distal domain assumes a proximal cell state and displays a duplicated proximal element: the notum (10). Furthermore, it has also been seen that proximal domain of the wing primordium can regenerate surgically ablated distal elements; however, a vice versa-type event does not take place (reviewed in ref. 11). These findings mirror progressive restriction of developmental

Significance

Not all cell types in a lineage hierarchy succumb to cancer in the face of an oncogenic lesion. What turns only select cells within an organ into "cells-of-origin" in cancer is an enduring riddle of cancer biology. Here we show that in epithelial primordia of adult wings and eyes of *Drosophila*, oncogenically mutated cells lose their developmental commitments and, instead, switch to a primitive or progenitor-like cell state. Switch-to-a-primitive-cell-state could thus be a prevalent mechanism of epithelial carcinogenesis and, possibly, an essential characteristic of cancer cells-of-origin.

Author contributions: S.J.K. investigated tissue surveillance and tumor cooperation; A.B. investigated links between cell fate regulation and neoplasia; M.A.A. investigated tumor cooperation; R.P.G. carried out transcriptional profiling of mosaic discs; S.H., R.K.P., and S.G.-B. contributed to early stages of work on tissue surveillance and tumor invasion; A.N. and A.M. investigated *scrib* induced neoplasia; and P.S. designed the investigation and wrote the paper.

The authors declare no conflict of interest.

This article is a PNAS Direct Submission.

Freely available online through the PNAS open access option.

Data deposition: The microarray data have been deposited in Array Express (http://www.ebi.ac.uk/arrayexpress/experiments/E-MEXP-2753/) (accession no. E-MEXP-2753).

[1]S.J.K., A.B., and M.A.A. contributed equally to this work.

[2]Present address: Department of Cell and Developmental Biology, University of Illinois at Urbana–Champaign, Urbana IL 61801.

[3]Present address: Molecular Biology Lab, Department of Pharmacology, Piramal Life Sciences, Goregoan (East), Mumbai 400 063, India.

[4]Present address: Department of Genetics, Dartmouth Medical School, Hanover, NH 03755.

[5]To whom correspondence should be addressed. E-mail: pradips@iitk.ac.in.

This article contains supporting information online at www.pnas.org/lookup/suppl/doi:10.1073/pnas.1212513110/-/DCSupplemental.

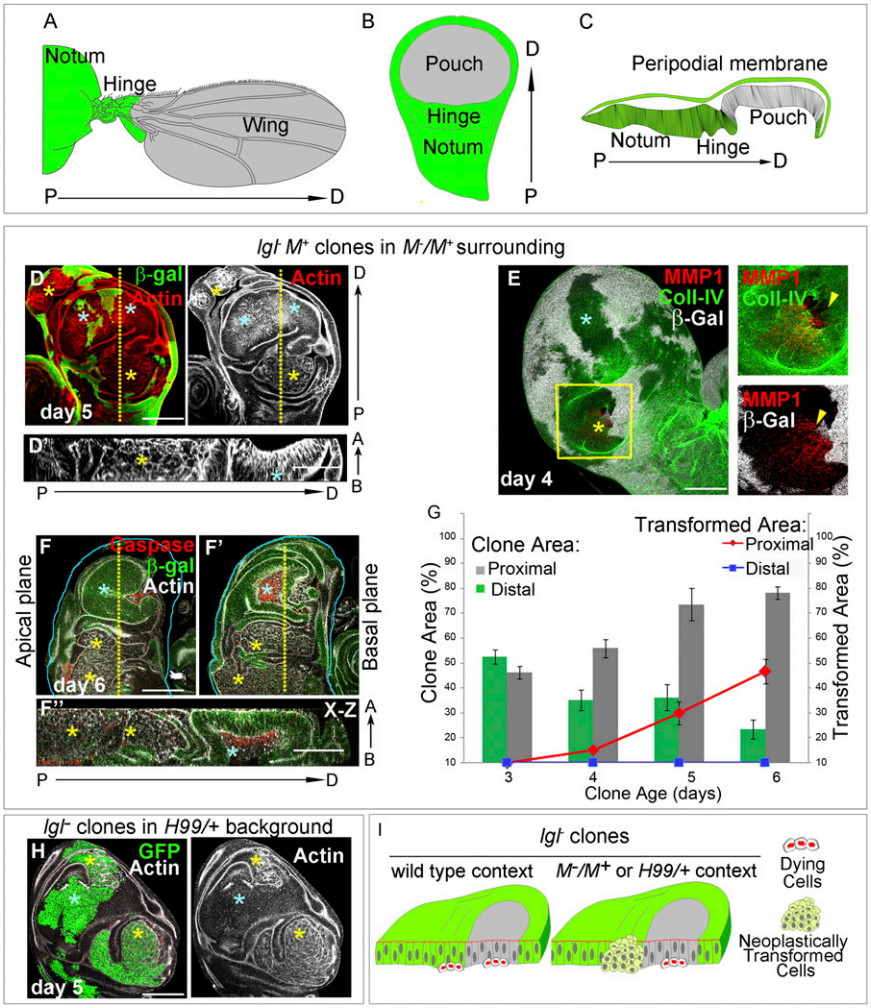

Fig. 1. Distinct neoplastic propensities of *lgl*$^{-}$ clones in proximal and distal wing imaginal disc epithelium. Cartoons of (*A*) an adult wing and (*B*) third-instar larval wing primordium. Notum and hinge (green) are parts of the proximal wing; wing pouch (gray) represents the distal wing blade. P→D designates proximal-distal axis. (*C*) Cartoon of lateral view of the wing imaginal disc epithelium, as seen in an optical section, displaying its proximal (green) and distal (gray) domains. (*D*–*G*) Images and data from mosaic discs where *lgl*$^{-}$ *M*$^{+}$ clones (absence of β-gal) are surrounded by cell competition compromised *M*$^{-}$/*M*$^{+}$ heterozygous cells. (*D*) Note that *lgl*$^{-}$*M*$^{+}$ clones in the distal domain (blue stars) do not transform neoplastically as revealed by their intact cytoarchitecture (actin, gray). Proximally (yellow stars), however, their altered cytoarchitecture reveals their neoplastic transformation. (*D*′) An *x*–*z* optical section along the yellow dotted line in *D* to reveal intact and altered cytoarchitecture of distal (blue star) and proximally neoplastic clones (yellow star), respectively. (*E*) Proximal clones (yellow star) shows expression of matrix metalloproteinase-1 (MMP1, red) and breakdown of the basement membrane, marked by collagen-IV-GFP (Coll-IV, green) while the distal clone (blue star) does not; absence of β-gal (gray) marks clone boundary. Higher magnifications of boxed area of *E* is shown at the far right column to reveal correspondence between disrupted basement membrane (Coll-IV, arrowhead) with MMP1 expression (red) within the clonal area (absence of β-gal, gray). (F–F′′) In older (day 6) mosaic discs, distal (blue star) *lgl*$^{-}$*M*$^{+}$ clones (absence of β-gal, green) were not seen in the apical plane (*F*), while in the basal plane (*F*′) these displayed extensive cell death (caspase, red). Optical section along the *x*–*z* plane (*F*′′) through the yellow dotted line shown in *F* and *F*′ reveals basal extrusion of these distal (blue star), caspase-expressing (red) clones. Note the abundant neoplastic transformation of proximal clones (yellow stars) in all of the three optical planes. A←B indicates the direction of of apical-basal polarity. (*G*) Plot of total and transformed clonal area of proximal and distal *lgl*$^{-}$*M*$^{+}$ clones in mosaic wing imaginal discs through successive days of clonal growth. (*H*) *lgl*$^{-}$ clones marked by GFP (green) and generated in a cell death compromised *H99*/+ genetic background. Distal clones (blue star) display intact cytoarchitecture (actin, gray) but proximally (yellow stars) these are neoplastically transformed. (*I*) Cartoon representation of *lgl*$^{-}$ clones in mosaic wing disc epithelium in different genetic contexts. Clonal age is shown as days after clone induction. (Scale bars, 100 μm.)

capacities in the proximal-distal lineage hierarchy of the wing primordia.

The eye imaginal disc of third-instar larva presents yet another model organ primordium, where cells of a developmental hierarchy representing distinct stages of retinal development are seen in spatially discrete domains (12). These organ primordia (wing and eye) therefore offer the advantage of spatial resolution of cells with distinct developmental capacities. Furthermore, in these epithelial primordia, cross-talks between a primary tumor (mutant cell) and its tissue microenvironment, namely the neighboring nontransformed cells, could be studied as well. A number of contact-dependent intercellular tissue microenvironmental surveillance (reviewed in refs. 13 and 14) mechanisms (subsequently referred to as tissue surveillance) has been suggested to restrain run away tumor growth in mammalian models. In *Drosophila* imaginal epithelia as well, tissue surveillance mechanisms, such as cell competition (15–18) and intrinsic tumor suppression (19), have been implicated in elimination of neoplastic mutant clones.

Here we have examined mutant somatic clones of a highly conserved tumor suppressor gene, *lethal giant larvae* (*lgl*), in the primordia of adult wings and eyes. Our results reveal that cell survival upon escape from tissue surveillance and gain of cooperative signaling pathways (or transcription factors) propel *lgl*$^{-}$ clones in both these organ primordia to lose their terminal cell fate commitments resulting in their switch to primitive cell states during the course of their tumor progression. In contrast, imposing a terminal cell fate commitment by gain of a field (wing) selector like Vg, for example, arrests neoplastic transformation of *lgl*$^{-}$ clones in the wing primordium and induces their large-scale cell death. Given the conservation of fundamental developmental and disease mechanisms, a ground rule of "switch-to-a-primitive-cell-state" seen during epithelial neoplasia in *Drosophila* is therefore likely to be of wider relevance in our understanding of cancer cells of origin and their pathogenesis.

Results

***lgl*$^{-}$ Somatic Clones of Proximal and Distal Wing Primordia Display Disparate Neoplastic Propensities.** Cell competition is a tissue-surveillance mechanism for organ homeostasis (reviewed in ref. 20). Somatic clones mutant for the *lgl* tumor suppressor gene (Fig. S1*B*), and also those of other *Drosophila* neoplastic tumor suppressors, are eliminated from mosaic imaginal disc epithelium by cell competition. Therefore, alleviation of cell competition in *lgl*$^{-}$ clones (and other neoplastic mutants) in a *Minute* (*M*$^{-}$/*M*$^{+}$) surrounding is permissive for their survival and eventual neoplasia (15–18) through successive days of their clonal growth (Fig. S1*C*). However,

despite growth and survival upon escape from cell competition-mediated elimination, these lgl^- (henceforth depicted as lgl^-M^+) clones displayed neoplastic transformation in only the proximal domain (Fig. 1*D*). Neoplastic transformation of these lgl^- clones is accompanied by: (*i*) loss of apico-basal polarity as assayed by mislocalization of either the actin cytoskeleton (18, 21) (Fig. 1*D*) or apical/lateral membrane markers, such as Discs Lost, Dlt (Fig. S1*D*) and, subsequently, (*ii*) by their invasive transformation, marked by breakdown of their basement membrane (Fig. 1*E*). Proximal-distal identity of these lgl^-M^+ clones could be readily ascertained by their characteristic epithelial folds (Fig. 1*D*) or by marking the proximal domain with Hth (Fig. S1*E*) (6, 7). However, despite a permissive tissue microenvironmental context, distal lgl^-M^+ clones were eliminated from the mosaic disc epithelium, after an initial period of survival, because of cell death (blue star in Fig. 1*F*), and were basally extruded from the wing epithelium (Fig. 1 *F′–F″*). In contrast, neoplasia in their proximal counterparts continued unabated (yellow stars in Fig. 1 *F–F″*); bulk of the neoplastically transformed lgl^- clones in mosaic wing imaginal discs therefore is of proximal origin (Fig. 1*G*). We also noted that basal extrusion of lgl^- clones and their cell death could not be arrested by expressing a baculovirus inhibitor of apoptosis, namely p35 (22) (lgl^- *UAS-p35* clones in Fig. S1*H*). Furthermore, distally extruded lgl^- clones also did not delaminate as revealed by their intact basement membrane (Fig. S1*G*). In these respects, extrusion of distal lgl^- clones seen here is distinct from mutant clones displaying genomic instability, which often delaminate and turn neoplastic when rescued from cell death by a gain of p35 (23).

Finally, because tissue surveillance-mediated elimination of disadvantaged cells invokes apoptosis, we further argued that a genetic compromise of cell death could rescue lgl^- clones from tissue surveillance as well. Heterozygosity for a deficiency, *Df(3L) H99* (*H99*/+, in brief), which deletes three closely linked proapoptotic genes—namely, *hid*, *grim*, and *reaper* (24)—is known to compromise cell death. We found that lgl^- clones generated in a *H99*/+ genetic background displayed distal survival and proximal transformation (day 5, Fig. 1*H*); however, in this genetic background as well, such as those in M^+/M^-, distal lgl^- clones displayed basal extrusion after day 5 of their induction (Fig. S1*F*). Taken together, these results reveal that neoplastic propensity of lgl^- clones is linked to their proximal-distal lineage hierarchy, distal being more resistant (Fig. 1*I*).

Multiple Signaling Pathways Can Cooperate for Proximal Neoplasia. Neoplastic transformation of somatic clones mutant for a given *Drosophila* tumor suppressor gene could be triggered by gain of cooperating signaling pathways (25, 26). Selective neoplastic transformations of lgl^- clones in the proximal wing primordium imply activation of such cooperating signaling pathways in this spatial domain. To obtain an unbiased view of these misregulated cellular signaling pathways, we performed genome-wide transcriptional profiling of mosaic wing primordia carrying proximally transformed lgl^-M^+ clones in an M^-/M^+ surrounding (for details, see Fig. S1) and compared them with that of control mosaic wing discs that carried M^+ clones, also generated in an M^-/M^+ surrounding (Fig. S1*I*). Thus, control and test mosaic discs differed primarily in terms of their clonal genotypes, surrounding cells being identical. We noticed twofold up- or down-regulation of 356 genes in test samples compared with control or baseline samples ($P \leq 0.05$) (Fig. S1*J*), besides tight correspondence among the biological replicates (Fig. S1*K*). Heat-maps of gene-sets of different signaling pathways also displayed broad agreements among their respective replicates (Fig. S1 *L–O*). However, to assess the status of different signaling pathways in these mosaic wing imaginal discs, we went beyond the fold-changes of individual genes and, instead, took a pathway centric approach using gene-set enrichment analysis (GSEA) (27), a statistical tool that uses an a priori-defined set of genes, to ascertain if these gene-sets are enriched in one biological state as compared with another. We noted enrichment ($P<0.05$) of several signaling pathways, suggesting their misregulation in proximally transformed lgl^- clones; these include Hippo, Wnt/Wg, TGF-β, and EGFR pathways (Fig. 2 *A–D*). Quantitative PCR of representative members of individual signaling pathways correlated with their transcriptional status in the microarrays (Fig. 2 *A*, *ii*, *B*, *ii*, *C*, *ii*, and *D*, *ii*). Finally, we noted that only proximally transformed lgl^- clones displayed cellular up-regulation of Hippo signaling targets (reviewed in ref. 9), such as, Expanded (Ex) (Fig. 2*E*) (see also ref. 28) and Wg (Fig. 2*F*) (see also ref. 29), also a ligand for Wg signaling (Fig. 2*F*).

To test if these signaling pathways enriched in transcriptional profiles of mosaic discs are functionally relevant for *lgl* neoplasia, we misregulated these signaling pathways, one at at a time, in lgl^- clones induced in a wild-type genetic background and asked if these would now override their elimination by tissue surveillance (see Fig. S1*B*). We misregulated Hippo signaling in lgl^- clones by inducing loss of Fat (Ft), a receptor of Hippo signaling; loss of Ft triggers nuclear translocation of Yki, resulting in activation of its target genes (reviewed in ref. 9). We noticed overproliferation and neoplastic transformation of lgl^- ft^- double-mutant clones in the proximal domain but distally these were eliminated (Fig. 2*A*, *iii*). Similarly, gain of Wg signaling in lgl^- clones induced by overexpression of Disheveled (Dsh), a down-stream transducer of Wg signaling (30), resulted in proximal neoplasia in lgl^- *UAS-dsh* clones, but distally these were eliminated by cell death (Fig. 2*B*, *iii*). Proximal neoplasia of lgl^- clones were also noted following gain of TGF-β or EGFR signaling pathways by expressing their respective activated receptors, namely Thick-veins (Tkv^{QD}) (Fig. 2*C*, *iii*) or EGFR ($EGFR^{\lambda top}$) (Fig. 2*D*, *iii*) but distally these were eliminated. Of note, individual misregulations of these signaling pathways, however, do not transform wing epithelial cells (Fig. S1 *P–S*).

Together, these results thus reveal that *lgl*-induced neoplasia in proximal domain of wing imaginal disc could be driven by misregulation of signaling pathways that are seen to be perturbed in transcriptional profiles of mosaic discs.

Rescue of Distal lgl^- Clones from Cell Competition and Cell Death Leads to Their Neoplastic Transformation. Distal elimination of lgl^- clones prevailed despite cooperation by signaling pathways (Fig. 2) or when cell death (*H99*/+) or cell competition (M^-/M^+) was individually compromised (Fig. 1). We thus asked if compromising both cell competition and cell death simultaneously would alleviate distal elimination of lgl^-M^+ clones generated in an M^-/M^+; *H99*/+ genetic context. Indeed, in such a context, where both cell competition and cell death are compromised, distal lgl^-M^+ clones were transformed (day 7, Fig. 3*A*) although onset of their neoplasia was substantially delayed (Fig. S2*A*).

In light of the above results, it thus appeared surprising that misregulation of most signaling pathways, particularly Hippo, which promotes growth and cell competition (9, 31), failed to override distal elimination of lgl^- clones (Fig. 2*A*, *iii*). It is, however, likely that the consequences of loss of Ft in distal and proximal domains of the wing disc were not similar, presumably because of its cross-talks with locally active morphogen signalings (32, 33). To overcome this limitation of dissimilar outcomes of loss of Ft in these two developmental domains, we overexpressed Yki in lgl^- clones under the ubiquitously active promoter of the *tubulin* gene. Indeed, unlike lgl^- ft^- clones (Fig. 2*A iii*), Yki overexpressing lgl^- clones (lgl^- *UAS-yki*) displayed massive overgrowth over the entire wing imaginal disc because of fusion of these fast-growing clones that obscured precise resolution of their proximal-distal origins (Fig. S2*B*). We thus reduced the duration of heat shock from 30 min to 4 min so as to induce only few dispersed clones to help resolve their proximal-distal spatial distribution. These discrete lgl^- *UAS-yki* clones, induced by a shorter heat pulse, were seen in both distal and proximal domains (Fig. 3 *B* and *C*). A closer examination revealed early signs of neoplasia in only some of these

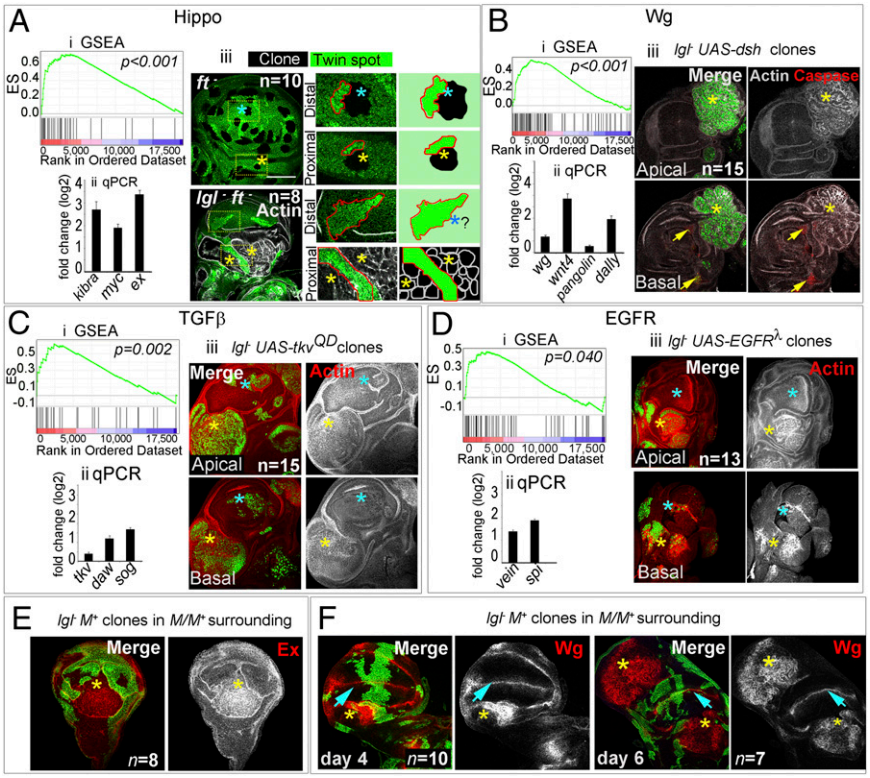

Fig. 2. Recruitment of multiple signaling pathways during proximal wing neoplasia. (*A–D*) Transcriptional status of Hippo (*A*), Wg (*B*), TGF-β (*C*), and EGFR (*D*) signaling pathways and their functional cooperation for *lgl*$^{-}$ neoplasia. (*A*, *i–D*, *i*) GSEA plots display enrichment of these pathways at $P < 0.05$; *y* axis displays enrichment score (ES) and *x* axis displays ranked order of genes in descending order of their fold-changes in *lgl*$^{-}$ vs. Wild-type; (*A*, *ii–D*, *ii*) Quantitative real-time PCR of representative members of the pathways show their up-regulation in *lgl*$^{-}$ mosaics. Error bars represent SEM. (*A*, *iii–D*, *iii*) Functional cooperation of individual signaling pathways for *lgl*$^{-}$ neoplasia; *n* represents the number of mosaic discs examined in each case. (*A*, *iii*) Functional cooperation of Hippo signaling: mosaic wing discs bearing *ft*$^{-}$ or *lgl*$^{-}$ *ft*$^{-}$ clones (loss of GFP). Distal (blue star) and proximal (yellow star) twin spots in boxed areas are shown at higher magnification in the *Center*; the far right panel shows their cartoon representation. Note that proximal and distal *ft*$^{-}$ clones outgrow their wild-type twins (dark green, red line). In contrast, distal *lgl*$^{-}$ *ft*$^{-}$ clones are conspicuous by their absence (question mark, blue star), but their wild-type twin-spot grew as expected. Proximal *lgl*$^{-}$ *ft*$^{-}$ clones display neoplastic transformation (actin, gray) and outgrow their wild-type twins (dark green). *lgl*$^{-}$ clones (GFP, green) overexpressing *UAS-dsh* (*B*, *iii*), *UAS-tkv*^{QD} (*C*, *iii*), and *UAS-EGFR*$^{\lambda top}$ (*D*, *iii*). Note that proximally all these clones (yellow stars) are transformed (actin) but distally (blue stars) these are rarely seen in the apical optical plane; however, basally these were invariably seen to be extruded. Mosaic disc in *B*, *iii* is marked for cell death (arrows, caspase, red), which are seen in the basal plane. (*E*) Selective up-regulation of Expanded, Ex (red) and (*F*) Wg (red) in proximally transformed *lgl*$^{-}$ clones (absence of green, yellow stars). Note that distally, where *lgl*$^{-}$ clones are not neoplastically transformed, Wg expression too was not altered in both 4- and 6-d-old clones (blue arrowheads). [Scale bar (applies to all panels), 100 μm.]

distal *lgl*$^{-}$ *UAS-yki* clones on the day 3 of clonal growth (Fig. 3*B*) although by this time many of their proximal counterparts were neoplastically transformed (Fig. 3*B*). Distal *lgl*$^{-}$ *UAS-yki* clones thus show a delayed onset of neoplasia. By day 4 of clone induction, however, the majority of the *lgl*$^{-}$ *UAS-yki* clones in both proximal and distal wing primordia were neoplastically transformed (Fig. 3*C*), while those that did not transform continued to display characteristics of nontransformed epithelial cells, namely, densely packed cells and compact nuclear morphology, as revealed by the nuclear GFP marker, besides their intact actin cytoarchitecture (arrow in Fig. 3*C*).

In summary, distal *lgl*$^{-}$ clones display neoplastic transformation (Fig. 3*D*) when their elimination is arrested by simultaneously compromising cell competition and cell death or when provided with a substantial advantage in cell proliferation or cell competition by gain of a cooperating partner, like Yki.

Loss of Wing Cell Fate During Neoplasia of Distal *lgl*$^{-}$ Clones. Proximal-distal disparity in neoplastic propensity could be linked to their respective lineage commitments. We thus asked if distally transforming *lgl*$^{-}$ clones retain their cellular memory by examining several exemplars of wing cell fate specification: namely, Vg (4), Distalless (Dll) (34), and Nubbin (Nub) (35). We considered *lgl*$^{-}$ *UAS-yki* clones ideal to examine this question because distally these are not eliminated (Fig. 3) and gain of Yki alone does not alter distal expression of these markers (Fig. 4 *A–C*). We noticed that down-regulation of Vg expression in *lgl*$^{-}$ *UAS-yki* clones sets in before the onset of neoplastic transformation (actin): that is, on the day 3 of clone induction (Fig. 4*D*). Furthermore, Vg is extinguished by the day 4 of clone induction (Fig. S2*C*), coinciding with neoplastic transformation of *lgl*$^{-}$ *UAS-yki* clones. Likewise, expressions of Dll (Fig. 4*E*) and Nub (Fig. 4*F*) were extinguished in distally transformed *lgl*$^{-}$ *UAS-yki* clones (day 4) as well. We also noticed loss of distal cell-fate marker, Dll, in mutant clones of another tumor suppressor, Scribble (Scrib) (21) (Fig. S2*D*); loss of cell fate could thus be prevalent during distal neoplasia.

The Yki transcription cofactor, in collaboration with one of its binding partner, Scalloped (Sd), a TEA-domain transcription factor, positively regulates *vg* transcription (36). Furthermore, feed-forward recruitment of Vg expression during expansion of the presumptive wing blade region because of Wg signaling too is Yki-mediated (8). Thus, loss of a terminal cell fate commitment in distal *lgl*$^{-}$ *UAS-yki* clones (Fig. 4*D*) is unlikely to be because of gain of a cooperative partner, like Yki; instead, it is likely to be a latent characteristic of transforming *lgl*$^{-}$ clone. To test this possibility, we examined expression of Vg in *lgl*$^{-}$*M*$^{+}$ clones generated in an *M*$^{-}$/*M*$^{+}$; *H99*/+ genetic context where these display distal survival and neoplasia (Fig. 3*A*) without the advantage of a forced gain of a cooperating partner, like Yki (Fig. 3 *B* and *C*). Early stage *lgl*$^{-}$*M*$^{+}$ clones (day 5 after clone induction, larval growth being slow in this genetic context) did not display a loss of Vg and were characterized by wiggly clonal borders (Fig. 4*G*), thereby revealing their normal cell-cell adhesion with the surrounding (also Vg-expressing) cells. Older *lgl*$^{-}$*M*$^{+}$ clones (day 7 after clone induction) (Fig. 4*H*) were of two types: (*i*) those that displayed early signs of down-regulation of Vg and showed smooth clone borders (yellow box, Fig. 4*H*), suggesting their cell fate changes (37); and (*ii*) those that were neoplastically transformed (blue box, Fig. 4*H*) and displayed complete loss of Vg, besides smooth clone borders. Loss of distal cell fate in *lgl*$^{-}$ clones therefore is a latent characteristic that manifests under conditions permissive for their survival.

Imposition of Wing Cell Fate in *lgl*$^{-}$ Clones Arrests Neoplasia and Induces Cell Death. In the wing primordium (Fig. 5*A*), Vg is regulated by inputs from two axial signaling cascades: N-Wg signaling

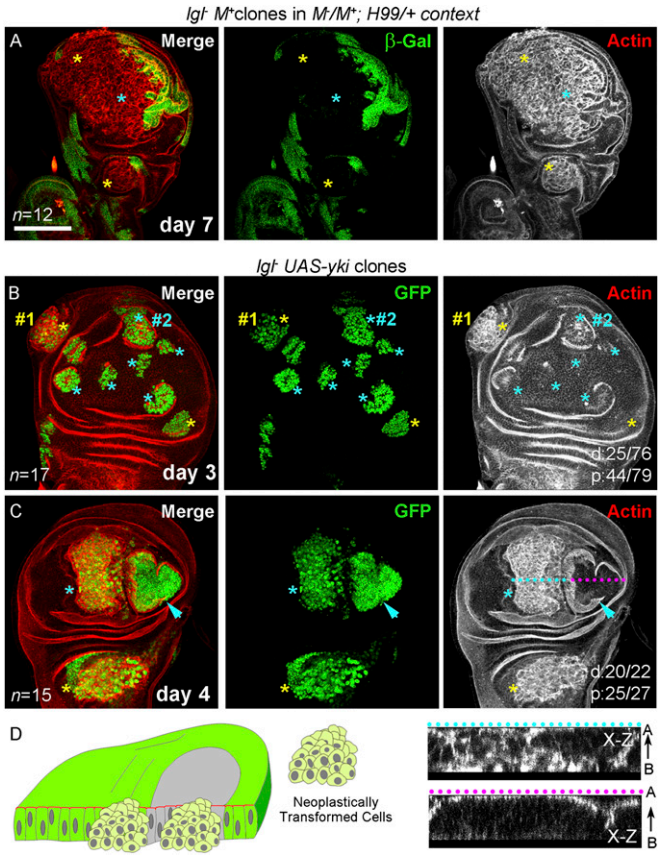

Fig. 3. Distal neoplasia of *lgl*⁻ clones under conditions that override their tissue microenvironmental surveillance and cell death. (*A*) *lgl*⁻ clones (absence of β-gal, green) in a genetic context compromising both cell competition (*M*⁻/*M*⁺) and cell death (*H99*/+) display neoplastic transformation (actin, red) in both proximal (yellow star) and distal (blue star) domains. (*B* and *C*) *lgl*⁻ *UAS-yki* clones (GFP, green) induced by a short pulse of heat shock (4 min). On day 3, only proximal clones are transformed (yellow star #1), but distal clone (blue star #2) display only early signs of actin reorganization (actin, red) (*B*). On day 4, proximal clones displayed neoplasia (yellows star) but distally one of the two large clones is neoplastically transformed (blue star), while other is not (arrow head) (*C*); optical sections along the *x*–*z* plane through the dotted line across transformed (blue) and nontransformed (pink) clones are shown at the bottom right panels to reveal altered F-Actin cytoarchitecture in only the former. (*D*) Cartoon representation of transformed *lgl*⁻ clones in both distal and proximal territories under conditions of reduced tissue surveillance and cell death. *n* = number of discs examined. Scores for distal (d) or proximal (p) clones showing neoplasia are displayed in the panel. A←B indicates apical-basal polarity. [Scale bar (applies to all panels), 100 μm.]

inputs from the Dorsal-Ventral (D/V) axis and decapentaplegic (Dpp) signaling inputs from the Anterior-Posterior (A/P) axis. N signaling activates a D/V boundary enhancer of *vg* (4), which is then maintained by Wg. Expression of Cut (Ct) (Fig. 5*A*), a neuronal cell fate marker on the D/V boundary (38), is also triggered by N signaling and is maintained by its cross-talks with Wg signaling (39). Furthermore, a combined N (4, 40) and Wg (35, 39) signaling and activities of Yki (8) positively regulate Vg expression in the wing pouch domain through its quadrant enhancer *(Q-vg)*. Finally, secreted Dpp signaling from the A/P axis too positively regulates the *Q-vg* enhancer (4).

Loss of Vg in neoplastic *lgl*⁻ clones (Fig. 4*D*) could thus be fallouts of down-regulation of these two A/P and D/V signaling inputs. To test these possibilities, we first examined expression of nuclear targets of these two axial signaling systems in distally transformed *lgl*⁻ *UAS-yki* clones. Spalt is a short-range Dpp signaling target and its expression is compromised when Dpp signaling is down-regulated along the A/P axis (41). Expression of Spalt, however, was not affected in *lgl*⁻ *UAS-yki* clones (Fig. S2*F*). Thus, apparently, Dpp signaling is not compromised in neoplastic *lgl*⁻ clones. In contrast, the N-Wg signaling target, Ct, is down-regulated in *lgl*⁻ *UAS-yki* clones ahead of their neoplastic transformation (boxed area, Fig. 5*B*) and is extinguished when these are neoplastically transformed (star, Fig. 5*B*). These results therefore suggest a down-regulation or perturbation in N-Wg signaling in distally transforming *lgl*⁻ *UAS-yki* clones. We thus sought to test if a gain of N or Wg signaling would restore expression of Vg in distal *lgl*⁻ clones. Gain of N, by expressing its activated receptor (N^{intra}) (4), in distal wing hindered clonal growth (Fig. S2*G*). This finding was not surprising because a high threshed of N signaling in developing wing disc at the D/V boundary corresponds to a zone of nonproliferating cells (4, 42). N activation in distal *lgl*⁻ clones (*lgl*⁻ *UAS-N*^{intra}) resulted in their elimination as well; however, proximally these were transformed (Fig. S2*H*) and could ectopically turn on its targets, like Dll (Fig. S2*I*). Clones displaying gain of Wg signaling (*UAS-dsh*) grew well in both proximal and distal domains (Fig. 5*C*). Furthermore, distally these inevitably displayed up-regulation of Vg (blue arrowheads, Fig. 5*C*) but, in contrast, proximally only about 10% of these clones showed ectopic gain of Vg (yellow arrowhead, Fig. 5*C*) (see also ref. 35). Gain of Wg signaling in distal *lgl*⁻ clones (*lgl*⁻ *UAS-dsh*), however, resulted in their elimination by

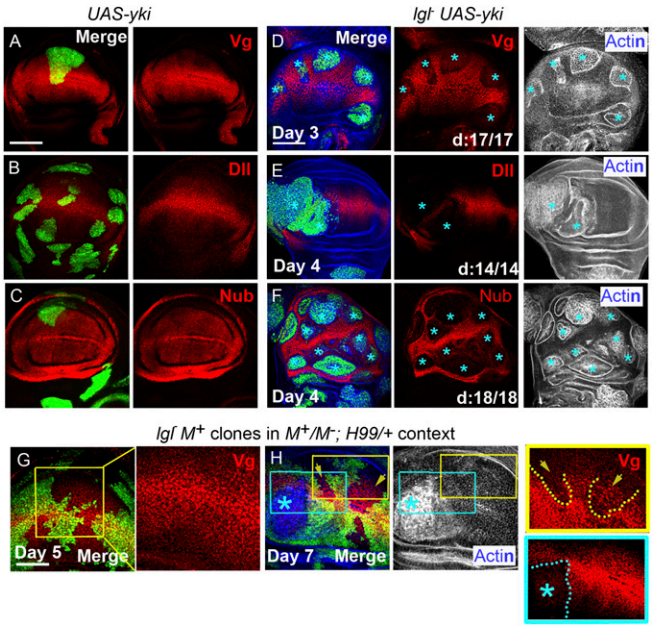

Fig. 4. Loss of cell fate during distal neoplasia of *lgl*⁻ clones. (*A*–*C*) Yki-expressing (*UAS-yki*, green) clones do not alter distal expression of Vg (*A*), Dll (*B*), or Nub (*C*) but (*D*–*F*) their *lgl*⁻ *UAS-yki* counterparts (GFP, green) do (blue stars). Distal *lgl*⁻ *UAS-yki* clones shown in *D* display intact cytoarchitecture (actin), whereas those shown in *E* and *F* are neoplastically transformed (actin). (*G* and *H*) Expression of Vg in *lgl*⁻*M*⁺ clones (loss of GFP, green) induced in a cell competition (*M*⁻/*M*⁺) and cell death (*H99*/+) compromised context. Boxed area in a mosaic distal wing imaginal disc, dissected day 5 after clone induction highlights wiggly clonal borders (*G*); Vg (red) expression in these clones, however, is not affected (shown at higher magnification). At a later stage of their growth, such clones display both neoplastically transformed (blue star) and nontransformed (yellow arrows) territories (*H*). Yellow boxed area is shown at a higher magnification at far right column to reveal clonal territory (yellow dotted lines), which are not transformed yet (actin, gray) but show down-regulation of Vg (arrowhead) and smooth clone border. Blue boxed area shown at a higher magnification (shown at the far right panel) display neoplasia (Actin, gray), loss of Vg (blue star), and smooth clone border (dotted blue line). Scores of distal (d) clones are also shown. (Scale bars, 100 μm.)

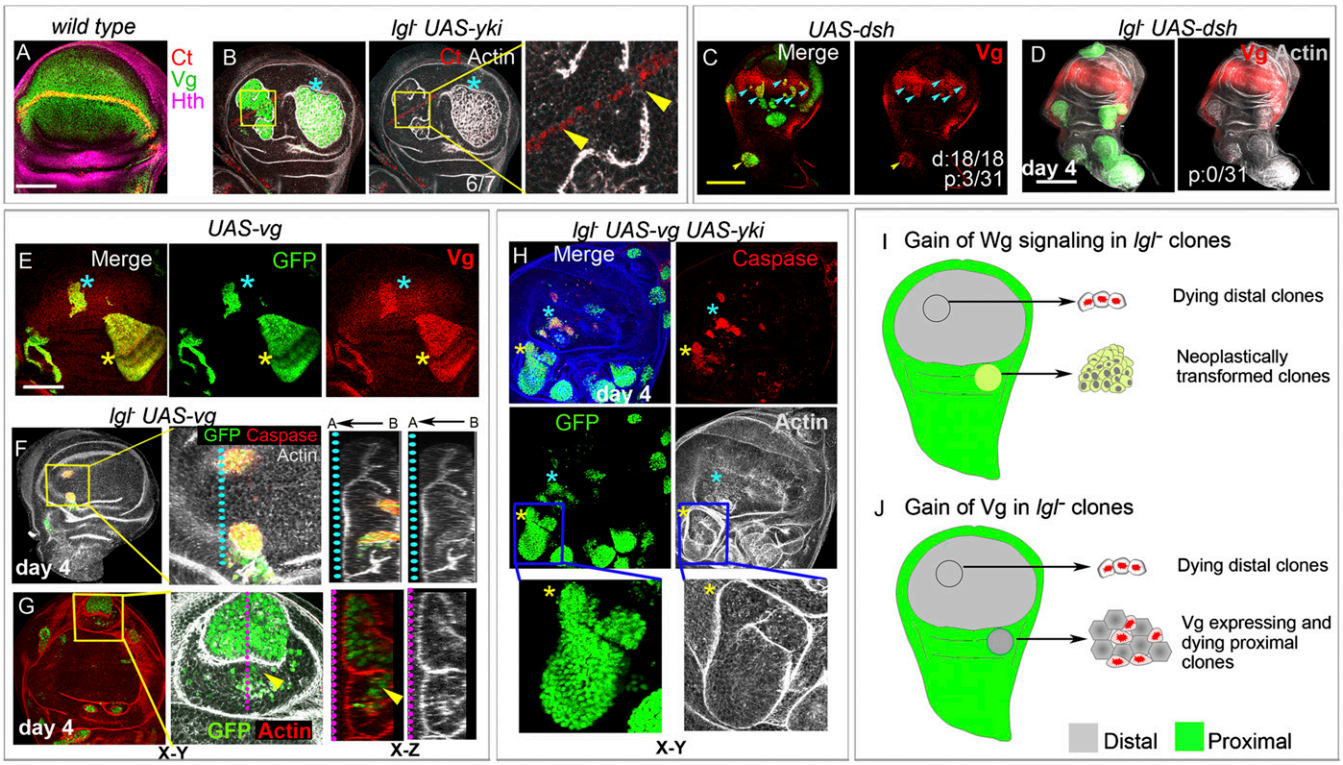

Fig. 5. Distal cell fate is incompatible with neoplastic cell state. (*A*) Wild-type third-instar wing imaginal disc displaying expressions of a N target, Ct (red) along the dorsal-ventral wing margin, and Vg (green) in distal wing (pouch domain); expression of Hth (purple) marks the proximal wing. (*B*) In a neoplastically transformed (actin, gray, blue star) distal *lgl*$^{-}$ *UAS-yki* clones (green) expression of Ct (red) is extinguished. Boxed area marks a nontransformed distal clone (actin, gray), which is shown at a higher magnification on the right to reveal early signs of loss of Ct (between the arrowheads). (*C* and *D*) Clones displaying gain of Wg signaling (*UAS-dsh*, green) activate Vg in distal (blue arrowheads) and in select proximal (yellow arrowhead) clones (*C*). In contrast, *lgl*$^{-}$ *UAS-dsh* (green) clones are not seen in the distal wing (marked by Vg, red, *D*); proximally (outside the domain of Vg, red, *D*) these are neoplastically transformed, but fail to display gain of Vg, unlike their *UAS-dsh* counterparts (*C*). (*E–H*) Gain of Vg (*UAS-vg*, green) does not affect growth or survival in distal (blue star) or proximal (yellow star) domains of the wing primordium (*E*). However, Vg-expressing *lgl*$^{-}$ clones (*lgl*$^{-}$ *UAS-vg*, green), are distally eliminated because of cell death (caspase, red, *F*), but those that displayed proximal survival were not transformed (*G*). Higher magnification of boxed area in *F* and *G* is shown at the right and *x–z* sections over the dotted line are shown at the far right. Apical-Basal (A←B) orientation in the *x–z* sections is shown. Note the dispersed distribution of the *lgl*$^{-}$ *UAS-vg* clones (GFP, green) in the periphery of this proximal clone (marked by yellow arrowhead, *G*) and their basal extrusion as revealed in the *x–z* section. Nonextruded *lgl*$^{-}$ *UAS-vg* cells at the center of the clone are not transformed, as revealed by their intact cytoarchitecture (actin). (*H*) *lgl UAS-vg; UAS-yki* (green) clones display cell death (caspase, red) both distally (blue star) and proximally (yellow star). Higher magnifications of proximal clones (marked by blue box) are shown at the bottom panel to reveal densely packed cells and their intact cyto-architecture (actin). (*I* and *J*) Schematic presentation of the outcome of gain of Wg signaling (*I*) or the Vg transcription factor (*J*) in *lgl*$^{-}$ clones. Note that distally, where Wg signaling induces Vg expression (see *C*, above), *lgl*$^{-}$ *UAS-dsh* clones are eliminated while those that are proximally transformed do not activate Vg (see *D*, above). Gain of Vg in *lgl*$^{-}$ clones, however, inevitably induces distal elimination while proximally these remain growth-compromised and die extensively (see *F–H*). Scores for distal (d) or proximal (p) clones showing a given phenotype (loss or gain of a marker or neoplasia) are displayed in respective panels. [Scale bar (*A*, *B*, and *E–J*), 100 μm, (*C* and *D*), 200 μm.]

the day 4 of clone induction (Figs. 2*B*, *iii* and 5*D*) following an initial and transient period of their survival when these showed gain of Vg (Fig. S2 *J* and *K*). In contrast, proximal *lgl*$^{-}$ *UAS-dsh* clones were extensively transformed (Fig. 2*B*, *iii*); however, none of these displayed gain of Vg (Fig. 5*D*), unlike their control *UAS-dsh* counterparts (Fig. 5*C*). It is therefore likely that proximal *lgl*$^{-}$ *UAS-dsh* clones displaying gain of Vg are preferentially eliminated (indeed, on day 2 after clone induction, proximal *lgl*$^{-}$ *UAS-dsh* clones displayed activation of Vg; see Fig. S2*K*). Cell survival and neoplasia in distal *lgl*$^{-}$ clones could thus be linked to loss of Vg. Conversely, signaling pathways which trigger expression of Vg may block neoplasia. To directly test this possibility we examined the consequences of an outright gain of Vg in *lgl*$^{-}$ clones. Control Vg-expressing clones (*UAS-vg*) grew well in both distal and proximal domains (Fig. 5*E*). In contrast, distal *lgl*$^{-}$ *UAS-vg* clones showed rapid elimination; thus, these were rarely recovered (6 of 24 mosaic discs) after day 4 of clone induction and appeared as small clusters of GFP-expressing cells displaying cell death and basal extrusion (Fig. 5*F*). Proximal survival of *lgl*$^{-}$ *UAS-vg* clones (Fig. 5*G*), on the other hand, appeared marginally better than their distal counterparts (Fig. 5*F*). However, these too displayed cell death (Fig. S2*L*) and basal extrusion (Fig. 5*G*). Of note, in none of these *lgl*$^{-}$ *UAS-vg* clones (n = 20) examined in 14 mosaic discs were neoplastically transformed (Fig. 5*G*).

We further examined the consequences of gain of Yki in *lgl*$^{-}$ *UAS-vg* clones. However, despite gain of Yki, distal *lgl*$^{-}$ *UAS-vg UAS-yki* clones were poorly recovered (10 of 20 discs) and showed extensive cell death (Fig. 5*H*). Proximally, *lgl*$^{-}$ *UAS-vg UAS-yki* clones displayed a somewhat improved survival than their distal counterparts (Fig. 5*H*). However, these too displayed high caspase activity (Fig. 5*H*) that appeared to offset their growth advantage because of gain of Yki. Most significantly, none (n = 30) of the proximal *lgl*$^{-}$ *UAS-vg UAS-yki* clones, of the 17 mosaic discs examined, were transformed till the day 4 of clone induction (Fig. 5*H*) and displayed dense cell packing and compact nuclear morphology, unlike their *lgl*$^{-}$ *UAS-yki* counterparts, which were inevitably transformed at this clonal age (see Figs. 3 and 4).

In summary, distal gain of Wg signaling or Vg transcription factor in *lgl*$^{-}$ clones produced identical outcome: both induced

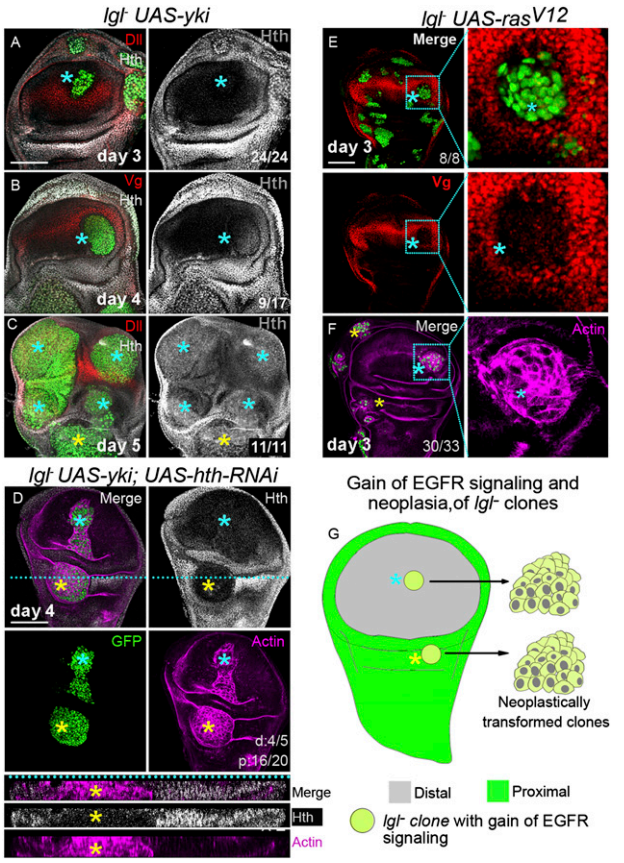

Fig. 6. Hth-independent neoplasia in *lgl*$^{-}$ clones in wing primordium. (*A–C*) *lgl*$^{-}$ *UAS-yki* clones (GFP, green) at different clonal age; Dll (*A* and *C*) and Vg (*B*) mark the distal domain. Note the progressive loss of these markers in distal *lgl*$^{-}$ *UAS-yki* clones (blue star) and gain of Hth (gray) on day 4 (*B*) and day 5 (*C*), but not on day 3 (*A*) of clone induction. Yellow star in *C* marks a proximal clone. (*D*) A proximal *lgl*$^{-}$ *UAS-yki; UAS-hth-RNAi* (GFP, green) clone (yellow star) displaying loss of Hth (gray); it is, however, neoplastically transformed such as its distal (blue star) counterpart (actin, purple). (*E–G*) Gain of Ras/EGFR signaling in *lgl*$^{-}$ clones represses distal cell fate and induces *lgl* neoplasia. *lgl*$^{-}$ *UAS-ras*^{V12} clones (GFP, green, *E*) on day 3 of clone induction repress Vg (red) and display neoplasia (actin purple, *F*); boxed areas in these images are shown at a higher magnification on their respective right panels. (*G*) Schematic representation of proximal and distal neoplasia in *lgl* clone upon gain of Ras/EGFR signaling. Scores displayed in *A–C*, *E*, and *F* are for distal clones while scores in *D* are for for distal (d) or proximal (p) clones. (Scale bars, 100 μm.)

cell death (Fig. 5 *I* and *J*). Proximally, however, these displayed two distinct outcomes: only those *lgl*$^{-}$ *UAS-dsh* clones were transformed neoplastically, which did not gain Vg, while their *lgl*$^{-}$ *UAS-vg* counterparts failed to transform neoplastically and displayed cell death (Fig. 5 *I* and *J*). Imposition of wing cell fate (gain of Vg, for example) in *lgl*$^{-}$ clones therefore blocks their neoplastic transformation, induction of cell death apart.

Neoplastic Cell State in the Wing Imaginal Disc is Hth-Independent. Roles of field selectors in cell fate determination (43) can be likened to binary switches: an ON state of Vg, for example, either because of its ectopic activation (4) or developmental regulation (44), imposes a wing cell fate by repressing or overriding a nonwing cell state. Loss of Vg (OFF state) in distally transforming *lgl*$^{-}$ clones would thus entail their reversal to a nonwing cell state. In order to test if distal *lgl*$^{-}$ clones assume a proximal-like cell state during clonal growth, expression of Hth, which is required for maintenance of proximal cell fate (6, 7), was examined. On the day 3 of clone induction—that is, prior to neoplastic transformation (Fig. 3*A*)—distal *lgl*$^{-}$ *UAS-yki* clones did not display a gain of Hth (Fig. 6*A*). On the day 4, only half of the distal *lgl*$^{-}$ *UAS-yki* clones displayed low-to-moderate gain in Hth expression (Fig. 6*B*), which was more pronounced in clones closer to the hinge region. Older (day 5) and distally neoplastic *lgl*$^{-}$ *UAS-yki* clones (see Fig. 3*D*) displayed uniform gain of Hth (blue star, Fig. 6*C*), matching their proximally transformed counterparts (yellow star, Fig. 6*C*).

It is thus likely that distally transformed *lgl*$^{-}$ clones, upon loss of Vg, acquire an Hth-dependent proximal-like cell state. In other words, Hth might cooperate for distal neoplasia of *lgl*$^{-}$ *UAS-yki* clones. We thus examined the consequences of misregulation of Hth in *lgl*$^{-}$ clones. *lgl*$^{-}$ clones expressing Hth (*lgl*$^{-}$ *UAS-hth*), however, are mostly eliminated from distal wing, although proximally these were neoplastically transformed (Fig. S3*B*). Hth therefore does not cooperate for distal neoplasia; this appears consistent with the observation that distal gain of Hth does not repress Vg (Fig. S3*A*) (7). Expectedly, down-regulation of Hth expression in *lgl*$^{-}$ clones (*lgl*$^{-}$*UAS-yki UAS-hth-RNAi* clones) did not affect distal neoplasia (blue star, Fig. 6*D*). However, surprisingly, these clones displayed proximal transformation, despite loss of Hth (yellow star, Fig. 6*D*). These results reveal that distal gain of Hth in *lgl*$^{-}$ clones (Fig. 6 *B* and *C*), or its persistent expression in proximal *lgl*$^{-}$ clones (Fig. 6*C*), are functionally redundant for neoplasia in the wing primordium. By extension, both distally and proximally transformed *lgl*$^{-}$ clones switch to cell states, which are Hth-independent.

Ras/EGFR Signaling Represses Vg and Induces Distal Neoplasia. Given the obligatory requirement of loss of Vg for *lgl* neoplasia (Figs. 4 and 5), it is likely that signaling pathways that negatively regulate Vg too could cooperate for distal neoplasia of *lgl*$^{-}$ clones. The Ras/EGFR signaling pathway, which regulates the choice of proximal cell fate in the developing wing primordium, might belong to this category of cooperative signaling partners for neoplasia in *lgl*$^{-}$ clones (5, 10); gain of EGFR signaling, for example, down-regulates Vg (Fig. S3*G*). However, because a gain of EGFR signaling in *lgl*$^{-}$ *UAS-EGFR*$^{\lambda top}$ clones did not induce distal neoplasia (Fig. 2*D*, *iii*), we sought to examine the consequences of gain of an activated Ras kinase (Ras^{V12}), which phenocopy homeotic functions of Ras/EGFR signaling in the wing primordium (5, 10). We thus examined the consequences of distal gain of Ras^{V12} in discrete *lgl*$^{-}$ *UAS-ras*^{V12} clones induced by a short pulse of heat shock (4 min) (Fig. 6*E*). These clones displayed repression of Vg (Fig. 6*E*), like their *UAS-ras*^{V12} counterparts (5). Furthermore, these clones were neoplastically transformed at a pace (day 3 of clone induction) matching that of their proximal counterparts (Fig. 6*F*). Control Ras^{V12}-expressing clones (*UAS-ras*^{v12}) on the other hand tend to sort out from their neighbors (Fig. S3 *C–E*), presumably as a consequence of a switch in their cell fate (37), but otherwise remained monolayered (45) and displayed intact cytoarchitecture (Fig. S3*C*). Thus, oncogenic cooperation of Ras^{V12} for distal neoplasia as seen here, and also those reported earlier (31), is likely to be aided by its ability to induce Ras/EGFR-mediated reversal of cell fate commitments (5) (summarized in Fig. 6*G*). Consistent with such a role of Ras/EGFR signaling for distal neoplasia, we further noticed that *lgl*$^{-}$ *UAS-EGFR*$^{\lambda top}$ clones too displayed distal neoplasia at an elevated growth temperature (29 °C) (Fig. S3*H*); a stronger Gal4 activity at 29 °C, may therefore elevate the level of *EGFR*$^{\lambda top}$, which is presumably required to for its distal cooperation during neoplasia of *lgl*$^{-}$ clones. In contrast, *lgl*$^{-}$ *UAS-tkv*^{QD} or *lgl*$^{-}$ *UAS-dsh* clones did not induce distal neoplasia at an elevated (29 °C) growth temperature (Fig. S3 *I* and *J*), consistent with the fact that gain of TGF-β or Wg signaling in distal wing would reinforce Vg cell fate, which is incompatible with a neoplastic cell state (Fig. 5).

It may be further noted that although Ras^{V12}-expressing clones display distal gain of Hth (Fig. S3*D*), presumably because of a loss of Vg, proximally it repressed Hth in the hinge domain (Fig. S3*E*).

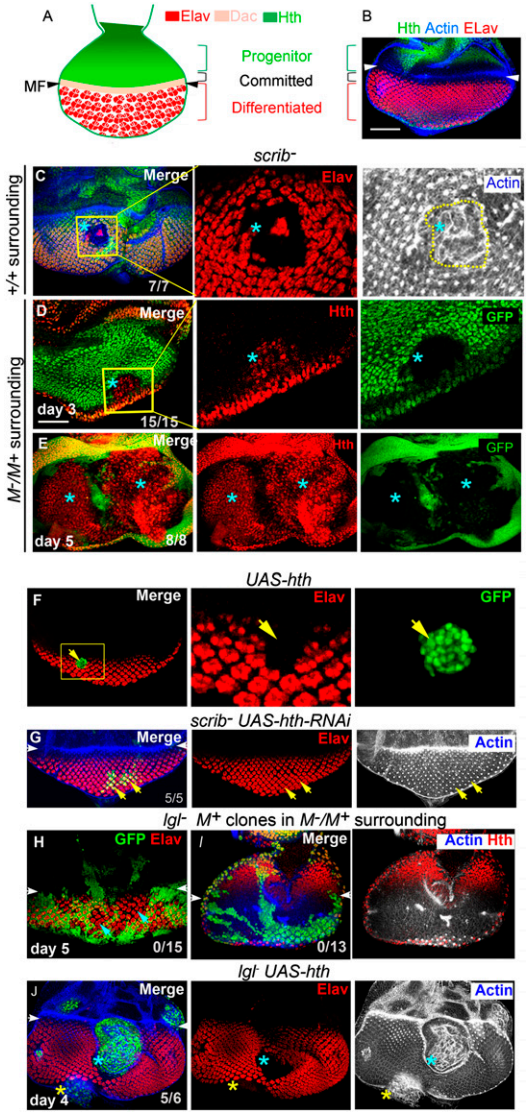

Fig. 7. Neoplastic cells of the eye primordium switch to an Hth-dependent progenitor-like cell state. (*A*) Cartoon of third-instar larval eye imaginal disc displaying three distinct stages of retinal development. The anterior-most progenitor cells express Hth (green) followed by a zone of Dac-expressing committed cells (peach) preceding the morphogenetic furrow (MF, arrowhead), which is succeeded by differentiated retinal cells (Elav, red). (*B*) An eye imaginal disc displaying domains of Elav and Hth expression. (*C*) *scrib*$^-$ retinal clone (loss of GFP, blue star). Boxed area in *C* is shown at a higher magnification on the right to reveal loss of Elav (red) in the clone and its neoplastic transformation (actin). (*D* and *E*) *scrib*$^-$*M*$^+$ clones (absence of GFP, blue star) generated in a *M*$^-$/*M*$^+$ surrounding. Boxed area in *D* is magnified on its right panels to display gain of Hth (red) on day 3 of clone induction (*D*). Expansion of clonal area on day 5 of clone induction results in near ubiquitous expression of Hth in the mosaic eye primordium. (*F–J*) Switch to a progenitor-like cell state drives neoplasia in the eye primordium. An *UAS-hth* clone (*F*, green) in the eye primordium; boxed area is shown on the right panels to reveal loss of Elav (red, arrow) corresponding to the domain of gain of Hth (GFP, green, arrow). *scrib*$^-$ *UAS-hth RNAi* clones (*G*, green, yellow arrows) do not lose Elav (red) and display characteristic ommatidial cytoarchitecture (actin, gray) and, thus, are no longer neoplastically transformed. In *lgl*$^-$ *M*$^+$ clones (loss of GFP, green), generated in *M*$^-$/M$^+$ surrounding, endogenous domains of Elav (red, *H*) or Hth (red, *I*) are not altered. In contrast, *lgl*$^-$ *UAS-hth* clones (green, blue star, *J*) display loss of Elav (red) and neoplastic transformation (actin, blue). The central large and neoplastically transformed clone (blue star) has popped out of the plane of the rest of the eye disc. The clone on the margin of the eye disc (yellow star) represents neoplastic transformation of margin cells. [Scale bar (for all panels), 100 μm.]

Furthermore, massively overgrown *lgl*$^-$ *UAS-ras*^{V12} clones spanning both distal and proximal domains display down-regulation of Hth (Fig. S3*F*). Thus, Ras^{V12}-mediated *lgl*$^-$ neoplasia in the wing primordium too, like those mediated by Yki (Fig. 6*D*), is Hth-independent.

Neoplastic Cell State in the Eye Primordium Is Hth-Dependent. Cell fate switch seen during neoplasia in the wing primordium could be a general feature of tumor progression in *Drosophila* epithelia. We examined this possibility in the eye imaginal disc where progenitors of the adult ommatidia (eye) and their derivatives are seen in discrete spatial domains. These include a domain of Hth-expressing eye progenitor cells, succeeded by a population of preproneural cells that are committed to retinal cell fate and marked by expression of transcription factors, like Dachshund (Dac) and Eyes absent (Eya), which is then followed by differentiated retinal cells marked by Elav (Fig. 7 *A* and *B*) (12).

Previously, it has been reported that *lgl*$^-$ retinal clones neither extinguish Elav nor transform neoplastically (18). Thus, we sought to examine the consequences of loss of *scrib* (21). In the eye disc, unlike their *lgl*$^-$ counterparts, *scrib*$^-$ clones displayed loss of Elav (red, Fig. 7*C*), and were neoplastically transformed (actin) (Fig. 7*C*) (16, 25, 46). Importantly, *scrib*$^-$ *M*$^+$ eye clones (in an *M*$^-$/*M*$^+$ surrounding) displayed an early gain of the retinal progenitor cell marker, Hth (day 3, Fig. 7*D*), which turned ubiquitous as the clonal territory expanded in the eye primordium (day 5; Fig. 7*E*). Previously, it has been shown that Hth expression arrests retinal cell differentiation by blocking Elav expression (47), as is evident in *UAS-hth* clones (Fig. 7*F*). Reversal in retinal cell differentiation and neoplasia in *scrib*$^-$ clones could thus be linked to their gain of Hth. If true, loss of Hth in *scrib*$^-$ eye clones would restore Elav expression. Indeed, *scrib*$^-$ *UAS-hth-RNAi* eye clones displayed expression of Elav (red, Fig. 7*G*) and restoration of their characteristic retinal cell architecture (actin, Fig. 7*G*). Given these findings in the *scrib*$^-$ clones (Fig. 7 *D* and *E*), we further argued that a persistent state of retinal differentiation in *lgl*$^-$ clones in the eye primordium (Elav, Fig. 6*H*) (18, 47) could be linked to their inability to recruit Hth activity (Fig. 6*I*), unlike their *scrib*$^-$ counterparts (Fig. 7 *D* and *E*). Conversely, gain of Hth should then render the retinal *lgl*$^-$ clones neoplastic. Indeed, gain of Hth in *lgl*$^-$ clones in the eye primordium (*lgl*$^-$ *UAS-hth* clones) resulted in their neoplastic transformation (Fig. 7*J*), reminiscent of their *scrib*$^-$ counterparts (Fig. 7*C*).

Taken together, these results reveal that neoplasia in an oncogenically targeted eye primordium sets in upon a cooperative gain of Hth that blocks or reverses their retinal cell differentiation, thereby switching to an Hth-dependent primitive/progenitor-like cell state.

Discussion

Switch-to-a-Primitive-Cell-State and Escape from Cell Death: A Framework for *Drosophila* Epithelial Neoplasia. Hallmarks of cancer, such as limitless replicative potential, escape from apoptosis or self-sufficiency in growth signals (reviewed in ref. 48) suggest subversion of normal developmental regulatory mechanisms during neoplastic growth. Developmental contexts that enable such neoplastic transformations, however, are not yet fully understood. By examining the consequences of loss of tumor suppressor genes in wing and eye primordia of *Drosophila*, we have herein asked if ontogeny of a mutated cell could foretell its neoplastic propensities. Although these two organ primordia display disparate developmental origins and their cell fates are specified by distinct sets of transcription factors, our results reveal a common paradigm of neoplasia: namely, their obligatory reversal to progenitor-like or primitive cell states, characterized by two hallmarks: first, reversal of their terminal cell fate commitments (loss of Vg and Elav in wing and eye, respectively), and second, gain/activation of transcription factors that are linked to primitive or progenitor-like

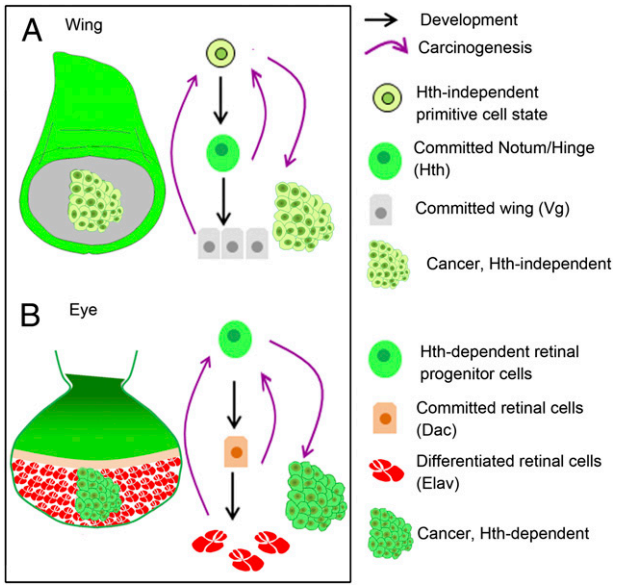

Fig. 8. Both lineage-committed and differentiated cells switch to primitive cell states during carcinogenesis. Cartoons of (*A*) wing and (*B*) eye discs displaying the cells which are committed to proximal (Hth), distal (Vg) wing, or retinal (Dac) cell fates or differentiated into retinal cells proper (red, Elav). Neoplastic transformations (irregular mass of cells) of these cells entail the following: first, loss of transcription factors that display their cell commitment (Vg) or differentiation (Elav) and, second, switch to a primitive/progenitor-like cell state (light green). Primitive cell state assumed by transformed *lgl*$^{-}$ clones in the wing is Hth-independent (*A*) while in the eye discs it is Hth-dependent (*B*).

developmental ground states (Fig. 8). Progression of an oncogenically targeted cell to a cancerous state therefore depends on its ability to recruit cellular partners, which promotes switch to a developmentally primitive cell state: for instance, by a gain of Ras/EGFR signaling in the distal wing or by a gain of a transcription factor, like Hth, in the eye primordium.

Carcinogenesis is also proposed to be an outcome of essentially two broad classes of cooperating events: first, oncogenic lesions that provide proliferative drive in mutated cells and, second, obligatory cellular cooperative events, such as genetic lesions or epigenetic changes in cooperating partners that ensure survival of the oncogenically targeted cells. Combination of these two cellular events culminate in escape of oncogenically targeted cells from cell death and, eventually, neoplasia (49, 50). We note that neoplasia of *lgl*$^{-}$ clones does not set in unless conditions permissive for their escape from cell death are available. Furthermore, loss of a terminal cell fate commitment (loss of Vg) is an essential requirement for escape from cell death as well, and thereby, neoplasia. Gain of Vg induces cell death in *lgl*$^{-}$ clones, both in the endogenous domain of its expression in distal wing (Fig. 5*F*) and outside: that is, proximal wing (Fig. 5*G*). These findings underscore primacy of cell fate reversal among the obligatory cellular events that cooperate for survival of the neoplastic cells. Loss of terminal cell fate and reversal to a primitive cell state are thus two intertwined cellular events that dictate cell survival and transformation of oncogenically targeted cells.

Primitive Cell States, Cancer Cells-of-Origin, and Context-Dependent Tumor Cooperation. Cells targeted by a neoplastic lesion are referred to as "cells-of-mutation," and those that finally display neoplastic transformation are called "cells-of-origin." All cells-of-mutation do not turn into cells-of-origin in cancer (2), an enduring reason for cell type-specific carcinogenesis. Cells-of-origin in cancer often tend to display stem cell-like characteristics; for example, crypt stem cells in intestinal epithelium that give rise to colorectal cancer (reviewed in ref. 2). Conversely, cells-of-mutation in breast epithelial cells tend to de-differentiate into a stem cell state before turning into cells-of-origin in breast cancer (51). Furthermore, in breast carcinoma, luminal cells with BRCA-1 mutation undergo basal-like cell fate switch before their neoplastic transformation (52). These and other examples notwithstanding, it is not yet clearly established if cells of origin in cancer are inevitably progenitor cell-like in nature or if lineage-committed or differentiated (nonprogenitor) cells too could turn into cancer cells-of-origin through reversals in their cell states. While our observations supports the latter alternative, namely switch in cell fates during tumor progression (Fig. 8), we also note that strategies for reversal in cell fate commitments are distinct in different developmental contexts. In the distal wing, for example, cellular reprogramming, exemplified by loss of Vg (Fig. 4, also see ref. 53), is a latent characteristic of *lgl*$^{-}$ clones that appears to be hastened by down-regulation of N-Wg signaling, or possibly by a concomitant gain of Ras/EGFR signaling. In the eye primordium, switch-to-a-primitive-cell-state is triggered by recruitment of Hth (Fig. 7), a regulator of progenitor cell state in the eye primordium (12, 47). Furthermore, our results reveal developmental context-dependent tumor cooperative roles of different signaling pathways (Figs. 2, 5, and 6) based on their ability to regulate local cell fates. For example, N, Wg, or Dpp (TGF-β) signalings, which promote a wing cell fate commitment (positive regulators of Vg), do not cooperate for neoplasia of *lgl*$^{-}$ clone in the distal wing (Figs. 2 and 5). Signaling pathways that promote neoplasia in one developmental context can thus suppress tumor progression in another.

Core Gene-Set for Primitive and Neoplastic Cell States. An intractable link between primitive and neoplastic cell states seen here is a pointer towards recruitment of a core gene-set in both these cell states. The transcription cofactor of the Hippo pathway, Yki, (reviewed in ref. 9), its target dMyc (54), and its partner Hth (12), are thus likely to be crucial members of this core gene-set. It has been previously shown that Yki is activated upon loss of Lgl (46, 55) or Scrib (16, 31) while its target dMyc is a driver of neoplasia in *lgl*$^{-}$ (17) and *scrib*$^{-}$ (16) mutant cells. Further, mammalian homolog of Yki, namely, transcriptional co-activator with PDZ-binding motif (TAZ), induces stem cell-like characteristic in breast epithelial cells transformed by loss of the Scrib (56). In *Drosophila* too, Yki is likely to be implicated in maintenance of stem cell-like characteristic: it is recruited in regenerating epithelial cells (55) and also plays a role in the maintenance of intestinal cell homeostasis (57). Furthermore, a Myc network has been shown to be an active component of both human embryonic stem cells and cancer cells (58). Hth, on the other hand, in collaboration with Yki, plays a critical role in the maintenance of retinal progenitor cells (12) which is likely to to be evolutionarily conserved (59). Further, recruitment of Hth during retinal cell neoplasia in *Drosophila* (Fig. 7) implicates this core gene-set in their switch to a progenitor-like cell state (Fig. 6). During normal course of development, Yki recruits different transcription factors, such as Hth (12), Sd (36), and Mad, the transcription factor of Dpp/TGF-β signaling pathway, in a developmental context-dependent manner (60). We note that neoplasia in the wing primordium is Hth-independent (Fig. 6), unlike that of the eye primordium (Fig. 7). In the wing primordium therefore Yki presumably partners with transcription factor(s) other than Hth to induce neoplasia. Rich genetics of the fly model could thus be explored to screen for these diverse sets of transcription factors with spatially distinct cooperative or tumor-suppressive roles in carcinogenesis.

Experimental Procedures

Genetic stocks of *Drosophila* were received from Bloomington *Drosophila* Stock Center, while antibodies were procured from Developmental Studies Hybridoma Bank or received as gifts from other investigators. Detailed material and methods are provided in *SI Experimental Procedures*.

ACKNOWLEDGMENTS. We thank L. Johnston, G. Morata, H. Bellen, G. Haldar, K. Basler, and the Bloomington *Drosophila* Stock Center for fly stocks; S. Cohen, H. Sun, S. Carroll, J. F. de Celis, and Developmental Studies Hybridoma Bank for antibodies; S. S. Pandey and S. Srivastava for technical help; A. Awadhiya for the illustrations; and P. Srivastava for critical comments on the manuscript. This work was supported by the financial assistance from a Department of Biotechnology's National Facility Grant and Research Council United Kingdom and Department of Science and Technology's United Kingdom-India Science Bridge grant (to P.S.); a Science and Engineering Research Council grant (to A.M.); the Indian Institute of Technology Kanpur support (to A.M.); and research fellowships from the Council of Scientific and Industrial Research (to S.J.K., M.A.A., R.P.G., and R.K.P.).

1. Barker N, et al. (2009) Crypt stem cells as the cells-of-origin of intestinal cancer. *Nature* 457(7229):608–611.
2. Visvader JE (2011) Cells of origin in cancer. *Nature* 469(7330):314–322.
3. Hariharan IK, Bilder D (2006) Regulation of imaginal disc growth by tumor-suppressor genes in *Drosophila*. *Annu Rev Genet* 40:335–361.
4. Kim J, et al. (1996) Integration of positional signals and regulation of wing formation and identity by *Drosophila* vestigial gene. *Nature* 382(6587):133–138.
5. Zecca M, Struhl G (2002) Control of growth and patterning of the *Drosophila* wing imaginal disc by EGFR-mediated signaling. *Development* 129(6):1369–1376.
6. Azpiazu N, Morata G (2000) Function and regulation of homothorax in the wing imaginal disc of *Drosophila*. *Development* 127(12):2685–2693.
7. Casares F, Mann RS (2000) A dual role for homothorax in inhibiting wing blade development and specifying proximal wing identities in *Drosophila*. *Development* 127(7):1499–1508.
8. Zecca M, Struhl G (2010) A feed-forward circuit linking wingless, fat-dachsous signaling, and the warts-hippo pathway to *Drosophila* wing growth. *PLoS Biol* 8(6):e1000386.
9. Pan D (2010) The hippo signaling pathway in development and cancer. *Dev Cell* 19(4): 491–505.
10. Wang S-H, Simcox A, Campbell G (2000) Dual role for *Drosophila* epidermal growth factor receptor signaling in early wing disc development. *Genes Dev* 14(18):2271–2276.
11. Bergantiños C, Vilana X, Corominas M, Serras F (2010) Imaginal discs: Renaissance of a model for regenerative biology. *Bioessays* 32(3):207–217.
12. Peng HW, Slattery M, Mann RS (2009) Transcription factor choice in the Hippo signaling pathway: Homothorax and Yorkie regulation of the microRNA bantam in the progenitor domain of the *Drosophila* eye imaginal disc. *Genes Dev* 23(19): 2307–2319.
13. Klein G (2009) Toward a genetics of cancer resistance. *Proc Natl Acad Sci USA* 106(3): 859–863.
14. Bissell MJ, Hines WC (2011) Why don't we get more cancer? A proposed role of the microenvironment in restraining cancer progression. *Nat Med* 17(3):320–329.
15. Agrawal N, Kango M, Mishra A, Sinha P (1995) Neoplastic transformation and aberrant cell-cell interactions in genetic mosaics of lethal(2)giant larvae (*lgl*), a tumor suppressor gene of *Drosophila*. *Dev Biol* 172(1):218–229.
16. Chen C-L, Schroeder MC, Kango-Singh M, Tao C, Halder G (2012) Tumor suppression by cell competition through regulation of the Hippo pathway. *Proc Natl Acad Sci USA* 109(2):484–489.
17. Froldi F, et al. (2010) The lethal giant larvae tumour suppressor mutation requires dMyc oncoprotein to promote clonal malignancy. *BMC Biol* 8:33.
18. Grzeschik NA, Amin N, Secombe J, Brumby AM, Richardson HE (2007) Abnormalities in cell proliferation and apico-basal cell polarity are separable in *Drosophila lgl* mutant clones in the developing eye. *Dev Biol* 311(1):106–123.
19. Igaki T, Pastor-Pareja JC, Aonuma H, Miura M, Xu T (2009) Intrinsic tumor suppression and epithelial maintenance by endocytic activation of Eiger/TNF signaling in *Drosophila*. *Dev Cell* 16(3):458–465.
20. Johnston LA (2009) Competitive interactions between cells: Death, growth, and geography. *Science* 324(5935):1679–1682.
21. Bilder D, Li M, Perrimon N (2000) Cooperative regulation of cell polarity and growth by *Drosophila* tumor suppressors. *Science* 289(5476):113–116.
22. Hay BA, Wolff T, Rubin GM (1994) Expression of baculovirus P35 prevents cell death in *Drosophila*. *Development* 120(8):2121–2129.
23. Dekanty A, Barrio L, Muzzopappa M, Auer H, Milán M (2012) Aneuploidy-induced delaminating cells drive tumorigenesis in *Drosophila* epithelia. *Proc Natl Acad Sci USA* 109(50):20549–20554.
24. White K, et al. (1994) Genetic control of programmed cell death in *Drosophila*. *Science* 264(5159):677–683.
25. Brumby AM, Richardson HE (2003) Scribble mutants cooperate with oncogenic Ras or Notch to cause neoplastic overgrowth in *Drosophila*. *EMBO J* 22(21):5769–5779.
26. Pagliarini RA, Xu T (2003) A genetic screen in *Drosophila* for metastatic behavior. *Science* 302(5648):1227–1231.
27. Subramanian A, et al. (2005) Gene set enrichment analysis: A knowledge-based approach for interpreting genome-wide expression profiles. *Proc Natl Acad Sci USA* 102(43):15545–15550.
28. Hamaratoglu F, et al. (2006) The tumour-suppressor genes NF2/Merlin and Expanded act through Hippo signalling to regulate cell proliferation and apoptosis. *Nat Cell Biol* 8(1):27–36.
29. Cho E, et al. (2006) Delineation of a Fat tumor suppressor pathway. *Nat Genet* 38(10): 1142–1150.
30. Neumann CJ, Cohen SM (1996) A hierarchy of cross-regulation involving Notch, wingless, vestigial and cut organizes the dorsal/ventral axis of the *Drosophila* wing. *Development* 122(11):3477–3485.
31. Menéndez J, Pérez-Garijo A, Calleja M, Morata G (2010) A tumor-suppressing mechanism in *Drosophila* involving cell competition and the Hippo pathway. *Proc Natl Acad Sci USA* 107(33):14651–14656.
32. Rogulja D, Rauskolb C, Irvine KD (2008) Morphogen control of wing growth through the Fat signaling pathway. *Dev Cell* 15(2):309–321.
33. Jaiswal M, Agrawal N, Sinha P (2006) Fat and Wingless signaling oppositely regulate epithelial cell-cell adhesion and distal wing development in *Drosophila*. *Development* 133(5):925–935.
34. Campbell G, Tomlinson A (1998) The roles of the homeobox genes aristaless and Distal-less in patterning the legs and wings of *Drosophila*. *Development* 125(22): 4483–4493.
35. Ng M, Diaz-Benjumea FJ, Vincent JP, Wu J, Cohen SM (1996) Specification of the wing by localized expression of wingless protein. *Nature* 381(6580):316–318.
36. Wu S, Liu Y, Zheng Y, Dong J, Pan D (2008) The TEAD/TEF family protein Scalloped mediates transcriptional output of the Hippo growth-regulatory pathway. *Dev Cell* 14(3):388–398.
37. Dahmann C, Basler K (2000) Opposing transcriptional outputs of Hedgehog signaling and engrailed control compartmental cell sorting at the *Drosophila* A/P boundary. *Cell* 100(4):411–422.
38. Jack J, Dorsett D, Delotto Y, Liu S (1991) Expression of the cut locus in the *Drosophila* wing margin is required for cell type specification and is regulated by a distant enhancer. *Development* 113(3):735–747.
39. Neumann CJ, Cohen SM (1997) Long-range action of Wingless organizes the dorsal-ventral axis of the *Drosophila* wing. *Development* 124(4):871–880.
40. Couso JP, Knust E, Martinez Arias A (1995) Serrate and wingless cooperate to induce vestigial gene expression and wing formation in *Drosophila*. *Curr Biol* 5(12): 1437–1448.
41. Nellen D, Burke R, Struhl G, Basler K (1996) Direct and long-range action of a DPP morphogen gradient. *Cell* 85(3):357–368.
42. Johnston LA, Edgar BA (1998) Wingless and Notch regulate cell-cycle arrest in the developing *Drosophila* wing. *Nature* 394(6688):82–84.
43. Carroll SB, Grenier JK, Weatherbee SD (2005) *From DNA to Diversity: Molecular Genetics and the Evolution of Animal Design* (Blackwell Scientific, Malden, MA), 2nd Ed.
44. Wu J, Cohen SM (2002) Repression of Teashirt marks the initiation of wing development. *Development* 129(10):2411–2418.
45. Karim FD, Rubin GM (1998) Ectopic expression of activated Ras1 induces hyperplastic growth and increased cell death in *Drosophila* imaginal tissues. *Development* 125(1):1–9.
46. Grzeschik NA, Parsons LM, Allott ML, Harvey KF, Richardson HE (2010) Lgl, aPKC, and Crumbs regulate the Salvador/Warts/Hippo pathway through two distinct mechanisms. *Curr Biol* 20(7):573–581.
47. Lopes CS, Casares F (2010) Hth maintains the pool of eye progenitors and its downregulation by Dpp and Hh couples retinal fate acquisition with cell cycle exit. *Dev Biol* 339(1):78–88.
48. Hanahan D, Weinberg RA (2000) The hallmarks of cancer. *Cell* 100(1):57–70.
49. Green DR, Evan GI (2002) A matter of life and death. *Cancer Cell* 1(1):19–30.
50. Lowe SW, Cepero E, Evan G (2004) Intrinsic tumour suppression. *Nature* 432(7015): 307–315.
51. Chaffer CL, et al. (2011) Normal and neoplastic nonstem cells can spontaneously convert to a stem-like state. *Proc Natl Acad Sci USA* 108(19):7950–7955.
52. Molyneux G, et al. (2010) BRCA1 basal-like breast cancers originate from luminal epithelial progenitors and not from basal stem cells. *Cell Stem Cell* 7(3):403–417.
53. Smith-Bolton RK, Worley MI, Kanda H, Hariharan IK (2009) Regenerative growth in *Drosophila* imaginal discs is regulated by Wingless and Myc. *Dev Cell* 16(6):797–809.
54. Neto-Silva RM, de Beco S, Johnston LA (2010) Evidence for a growth-stabilizing regulatory feedback mechanism between Myc and Yorkie, the *Drosophila* homolog of Yap. *Dev Cell* 19(4):507–520.
55. Sun G, Irvine KD (2011) Regulation of Hippo signaling by Jun kinase signaling during compensatory cell proliferation and regeneration, and in neoplastic tumors. *Dev Biol* 350(1):139–151.
56. Cordenonsi M, et al. (2011) The Hippo transducer TAZ confers cancer stem cell-related traits on breast cancer cells. *Cell* 147(4):759–772.
57. Ren F, et al. (2010) Hippo signaling regulates *Drosophila* intestine stem cell proliferation through multiple pathways. *Proc Natl Acad Sci USA* 107(49):21064–21069.
58. Kim J, et al. (2010) A Myc network accounts for similarities between embryonic stem and cancer cell transcription programs. *Cell* 143(2):313–324.
59. Bessa J, et al. (2008) meis1 regulates cyclin D1 and c-myc expression, and controls the proliferation of the multipotent cells in the early developing zebrafish eye. *Development* 135(5):799–803.
60. Oh H, Irvine KD (2011) Cooperative regulation of growth by Yorkie and Mad through bantam. *Dev Cell* 20(1):109–122.